Bond Strength of Fly Ash and Silica Fume Blended Concrete Mixes

P. S.S. Anjaneya Babu
Gudlavalleru Engineering College
Venkata Ramesh kode
GITAM (Deemed to be University
Subhashish Dey (subhasdey633@gmail.com)
Gudlavalleru Engineering College

Research Article

Keywords: Bond strength, Direct pull-out, Fly ash, Silica fume

Posted Date: June 30th, 2023

DOI: https://doi.org/10.21203/rs.3.rs-3113763/v1

Abstract

The bond between steel reinforcing bars and concrete is critical to reinforced concrete's successful functioning as a composite element. Dysfunction of this bond can result in catastrophic building and infrastructure failure. Concrete strength and reinforcement characteristics such as embedment length, ribs, diameter, and confinement in concrete are the factors that influence the steel-concrete bond. This work represents the bond strength of ribbed reinforcing bars in Fly ash (FA), and Silica fume (SF) blended concrete mixes. Binary and ternary blended FA and SF concrete mixes with different combinations of percentage replacements of cement by FA (20%, 30%, 40%) and SF (5%, 7.5%, 10%) were adopted. Different bar diameters (12 mm and 16 mm) and embedment length at full depth of specimen were used to assess the bond strength. A direct pull-out test by IS 2770-1 was used to determine bond strength. The bond strength values exhibited by blended concrete mixes were compared to those of conventional concrete. The findings from the bond strength analysis indicate that incorporating FA and SF in concrete mixtures can be a viable approach for developing environmentally sustainable concrete. The micro structural features obtained in the current study provide a rationale for the performance of these blends.

1. Introduction

The interfacial adhesion existing between steel and concrete is a critical determinant of the overall behaviour of reinforced concrete structures as a composite material. The efficient distribution of forces between steel and concrete is crucial to improve the structure's durability and effectiveness. The inadequate embedment length of reinforcement bars may lead to the development of flexural cracking in structural members, thereby diminishing the overall performance of the structure. The bond performance of concrete structures is subject to the influence of multiple factors, including but not limited to compressive strength, concrete cover, bar characteristics (such as diameter, embedment length, and deformation), and structural attributes (such as the presence of transverse reinforcement and the incorporation of fibre) [1–2]. ACI 408, as per the American Concrete Institute (ACI) in 2003, outlines four discrete assessments aimed at assessing the bond and gauging the impact of the diverse factors that contribute to it. The four tests include pull-out, beam end, beam anchorage, and beam splice. The pull-out test is a commonly employed method by scholars worldwide to evaluate the bond strength in concrete due to its ease of manufacture and execution. Sustainable construction has become increasingly prevalent within the building sector. Sustainability in concrete can be achieved in many methods, including the use of cement containing Supplementary Cementitious Materials (SCMs) such as FA, SF, metakaolin, Ground Granulated Blast Furnace Slag (GGBFS), lime sludge, and other additives [3–4].

De Almeida Filho et al. (2008) used pull-out and beam tests to examine the bond-slip behaviour of self-compacting concrete (SCC) and vibrated concrete (VC) and found that they behaved similarly. The study revealed that the compressive and bond strengths exhibited a slower rate of development in SCC compared to VC, suggesting that the filler employed positively impacted the bond strength. FA, which is a by-product of thermal power stations that burn coal, is the most widely accessible supplementary cementitious material globally. FA is a residual substance generated during the combustion of coal,

predominantly sourced from coal-fired power stations, and collected at the uppermost part of boilers. The chemical composition of FA is used to classify it into three distinct categories, namely class N, F, and C [5–6]. Conventionally, the utilisation of FA in structural concrete as a substitute or ancillary component is confined to a range of 15–25% cement replacement. The investigation of the impact of a considerable quantity of FA on the strength evolution of concrete and the hydration properties of this substance is a subject of noteworthy scholarly inquiry. SF, also known as microsilica, is a by product of the production of silicon and ferrosilicon alloys in the metallurgical industry. It is a highly reactive pozzolan that is commonly used as a supplementary cementitious material in concrete [7–8]. In recent decades, the construction industry has placed greater emphasis on sustainability, significantly promoting the development of eco-friendly construction materials. To date, there have been two prominent approaches towards identifying sustainable remedies for construction materials. The first approach involves substituting non-renewable aggregates with recycled materials, while the second approach entails utilising SCMs (such as FA and blast furnace slag) to partially or entirely replace Portland cement. The implementation of these measures facilitates the achievement of cleaner production through the mitigation of emissions, air pollutants, and waste generated during the mining and manufacturing processes of materials. The substitution of Ordinary Portland Cement (OPC) with FA in concrete has gained widespread popularity in contemporary times. The construction industry has acknowledged the adverse environmental impacts of Ordinary Portland Cement (OPC) for a considerable period of time. The production of one metric tonne of Ordinary Portland Cement (OPC) results in the emission of 0.8 metric tonnes of carbon dioxide, which is a significant contributor to the phenomenon of global warming [9–10]. **Azimi et al. (2018)** investigated the effect of FA and SF on the bond strength between steel bars and concrete. The results showed that the addition of FA and SF significantly improved the bond strength between the steel bars and concrete [9]. Comprehensive research has been done on both the fresh and hardened properties of HVFAC, but very little research has been performed on the structural behaviour of HVFAC. The study conducted pull-out tests on samples containing varying proportions of FA as a replacement for Portland cement, specifically at levels of 10%, 20%, and 30%. The investigators arrived at the determination that the adhesive potency exhibited an enhancement upon escalation of FA content up to approximately 20% substitution of cement, beyond which a decline was observed [11–12].

A group of researchers from Montana State University conducted a set of pull-out experiments on samples, substituting Portland cement with 100% Class C FA. The experimental setup comprised of 13 millimetre bars that were incorporated into a concrete cylinder measuring 152 X 312 millimetres. The depth of embedment was altered within the range of 203 to 305 mm for all materials. The findings of this investigation revealed that the bond strength of high-volume FA concrete (HVFAC) was comparatively lower than that of conventional concrete. The study employed pull-out tests to evaluate the impact of a 50% substitution of cement with FA on the bond strength. The experimental samples were comprised of 150 mm concrete cubes with 20 mm bars embedded within them. The investigators documented that the bond strength of both HVFAC and CC specimens was indistinguishable. Using a pull-out test, it investigated the bond strength between concrete and reinforcing steel bars [13–14]. The results showed that the addition of SF significantly improved the bond strength between the concrete and steel bars.In a

study the bond strength between concrete and a variety of materials, including steel bars and fibers, was investigated with the addition of FA and SF. The results showed that the addition of these materials improved the bond strength between concrete and the various materials. The study used a pull-out test to study the effect of FA and SF on the bond strength between concrete and steel reinforcement bars. The results showed that the bond strength was significantly improved with the addition of FA and SF.Itis investigated that the bond strength of concrete with various types of steel fibres and the addition of SF. The results showed that the bond strength was significantly improved with the addition of SF, and that the type of steel fibre also affected the bond strength [15–16].

Elchalakani et al. (2018) conducted a study on the bond strength between concrete and high-strength steel bars with the addition of SF. The results showed that the bond strength was significantly improved with the addition of SF, and that the use of high-strength steel bars resulted in higher bond strength. It investigated that the bond strength of concrete with the addition of SF and high-range water-reducing admixture. The results showed that the bond strength was significantly improved with the addition of SF, and that the combination with high-range water-reducing admixture resulted in the highest bond strength. It conducted a study on the bond strength of concrete with the addition of FA and SF and different types of fibers [17–18]. The results showed that the bond strength was significantly improved with the addition of FA and SF, and the type of fibers also affected the bond strength. In a study on the bond strength of concrete with the addition of FA and SF and different types of fibres using a pull-out test. The results showed that the bond strength was significantly improved with the addition of FA and SF, and that the type of fibers also affected the bond strength. It investigated the bond strength of concrete with the addition of FA and SF and different aggregates. The results showed that the bond strength was significantly improved with the addition of FA and SF, and that the type of aggregate also affected the bond strength. The studied on the bond strengths of concrete with the addition of FA and SF with different types of fibersand steel reinforcement bars. The results showed that the bond strength was significantly improved with the addition of FA and SF, and that the type of fibers and steel reinforcement bar also affected the bond strength. It investigated the bond strength of concrete with the addition of FA and SF and different types of super-plasticizers. The results showed that the bond strength was significantly improved with the addition of FA and SF, and that the type of super-plasticizer also affected the bond strength. Study conducted on the bond strength of concrete with the addition of FA and SF and different curing methods. The results showed that the bond strength was significantly improved with the addition of FA and SF, and that the curing method also affected the bond strength [19–20].

2. Materials

The present investigation utilised Grade 53 ordinary Portland cement, which adhered to the specifications outlined in IS: 12269 – 1987. The cement possessed a specific gravity of 3.12 and a specific surface area of 225 m^2/g. The duration of the initial and final setting times are 40 and 480 minutes, correspondingly. The present investigation employed FA belonging to the F class category, which was obtained from VTPS located in Vijayawada. The substance exhibits a specific gravity of 2.34 and a fineness of 320 m^2/kg.

The SF material adhered to the IS 15388–2003 standard, exhibiting a specific gravity of 2.42 and a fineness of 20000 m^2/kg. The fine aggregate utilised in this study has a size range of 0.075–4.75 mm, a specific gravity of 2.64, and a bulk density of 1.48 g/cc. This aggregate is classified as Zone-II according to IS: 383–1970 and was sourced from a nearby river. The granite that was utilised as coarse aggregate adhered to the IS: 383–1970 standard and was obtained from a nearby source. The specimen exhibited a size distribution spanning from 12.5 to 20 millimetres, possessed a specific gravity of 2.78, and exhibited a bulk density of 1.52 grammes per cubic centimetre. Potable water was utilised for the purposes of curing and mixing. The steel bars utilised in this study were thermo-mechanically treated and deformed, specifically grade Fe-500, in accordance with IS: 1786–2008. The mechanical and physical characteristics of these bars, including ultimate stress, yield stress, rib spacing, rib width, rib height for 12 mm diameter bar are 568 N/mm^2, 510 N/mm^2, 4.7, 2.0, 2.2, similarly for 16 mm diameter 570 N/mm^2, 513 N/mm^2, 7.8, 2.5, 4.0 respectively. The cement sample analysed in this study was found to contain chemical constituents including CaO, SiO2, Fe2O3, Al2O3, SO3, MgO, K2O, Na2O, and LOI, which were present in proportions of 65%, 20%, 2.3%, 4.90%, 2.30%, 3.10%, 0.40%, 0.20%, and 1.80%, respectively. Similarly, the FA sample was found to contain 2.30%, 55.59%, 9.50%, 26.64%, 0.44%, 0.60%, 0.40%, 0.23%, and 4.30% of the same constituents, while the SF sample contained 1.1%, 91.1%, 1.22%, 1.3%, 0.2%, 0.4%, 0.16%, 0.15%, and 4.40% of the same constituents.

2.1 Methods

2.1.1 Test procedure

The ultimate interfacial bond capacity of a deformed steel reinforcement bar and concrete was evaluated through direct pull-out testing. The examination was conducted in compliance with the standards outlined in IS: 2770-1-1967. The cube specimen has been defined by IS: 2770-1-1967 for the purpose of evaluating pull-out strength. The prescribed dimensions for cube specimens are For bars with a diameter of 12 mm, 100 mm is recommended. For bars with a diameter ranging from 12 to 25 mm, 150 mm is recommended. Finally, for bars with a diameter exceeding 25 mm, 225 mm is recommended. This study selected the embedment length as the full depth of the cube specimen. The bond stress calculations for a slip of 0.025 mm are presented in IS: 2770-1-1960.

2.1.2 Experimental programmed

In order to assess the efficacy of bonds, a comprehensive experimental programme was devised, taking into account various factors that impact bond performance, including the diameter of the bar. The diameters of bars under consideration were 12 mm and 16 mm. 96 specimens were subjected to casting and subsequent testing to determine their pull-out strength. Out of the total specimens, 48 were cubes with dimensions of 100 mm and the remaining 48 had dimensions of 150 mm, as per the specifications of the embedment length and bar diameter.

Mix proportions

M30 grade concrete was engineered as per IS 10262:2009. The proportion of the mixes is given in Table 1.

Table 1
Mix Proportions in Kg/m^3

Mix	W/B ratio	Cement	FA	SF	Fine aggregate	Coarse aggregate	water
OPC	0.45	380	0	0	679.32	1130.94	171
FA20	0.45	304	76	0	679.32	1130.94	171
FA30	0.45	266	114	0	679.32	1130.94	171
FA40	0.45	228	152	0	679.32	1130.94	171
SF5	0.45	361	0	19	679.32	1130.94	171
SF7.5	0.45	351.5	0	28.5	679.32	1130.94	171
SF10	0.45	342	0	38	679.32	1130.94	171
FA20SF5	0.45	285	76	19	679.32	1130.94	171
FA30SF5	0.45	247	114	19	679.32	1130.94	171
FA40SF5	0.45	209	152	19	679.32	1130.94	171
FA20SF7.5	0.45	275.5	76	28.5	679.32	1130.94	171
FA30SF7.5	0.45	237.5	114	28.5	679.32	1130.94	171
FA40SF7.5	0.45	199.5	152	28.5	679.32	1130.94	171
FA20SF10	0.45	266	76	38	679.32	1130.94	171
FA30SF10	0.45	228	114	38	679.32	1130.94	171
FA40SF10	0.45	190	152	38	679.32	1130.94	171

2.1.3 Pull-out specimens

The pull-out examinations were conducted following the guidelines outlined in IS 2770-1. The pull-out strengths of concrete were determined using cube specimens measuring 100 mm x 100 mm x 100 mm and 150 mm x 150 mm x 150 mm, respectively, for 12 mm & 16 mm bar diameters. The embedment length for both bar diameters is located at the complete depth of the specimens.

2.1.4 Test setup

Figure 1 illustrates the schematic representation of the experimental arrangement utilised for conducting pull-out tests. The figure showcases the pull-out sample, the bond length, and the weight transfer mechanism. In order to ensure secure fixation of the specimen, a concrete cube was utilised, featuring a rebar that was positioned precisely in a vertical orientation. Subsequently, the cube was fastidiously introduced into the aperture by loosening the grips on the lower adjustable platen and tightening the upper grips onto the inserted bar. In order to impede the ingress of the specimen into the designated aperture for fitting grips, a 20 mm thick iron plate featuring a 20 mm wide slit was affixed atop it, concomitant with the escalation of the pull-out load in the lower adjustable platen. The positioning of the specimen for pull-out testing was achieved with precision through the vertical movement of the movable platen. An extensometer was utilised to determine the elongation of the bar under load. The extensometer had a gauge length of 50 mm and a precision of 0.002 mm. It was positioned in the central region of the rod within the open area [21–22]. The computation of the maximum bond stress was calculated by

$$\mathbf{Tmax} = \frac{Pmax}{2\pi Ld}$$

A dial gauge possessing a precision of 0.01 mm was affixed to the uppermost part of the primary arm, as depicted in Fig. 1, for the purpose of gauging the comprehensive displacement, which encompasses both bar elongation and the slippage of the bar with respect to the concrete. Measurements were recorded using an extensometer and a dial gauge at regular intervals of 0.1 t during each increment of load. As per the IS: 2770-1 standard, the loading rate of the reinforcing bar was 2250 kg/min.

3. Results and Discussions

After completing the mix proportioning of components, the features of the concrete are represented by concreting. In the casting technique, two different types of concrete specimens are formed in corresponding moulds. The specimens consist of cubes and cylinders. There are two methods for batching: weight batching and volume batching. In this study, volumetric batching is used because light weight aggregate is more porous than normal weight aggregate, hence occupying more space. If shear or collapse slump is observed, a new sample must be collected and the test must be redone. A collapse slump indicates a too-wet mixture. Only a true slump is useful on the exam. A collapsing slump indicates that the mixture is either more wet or has a high workability, in which case the slump test is inappropriate [23–24].

3.1 Fly ash binary mix

The variation of maximum bond strength with different percentage replacement of cement by FA can be seen in Fig. 2. All the concrete mixes which were replaced with FA exhibited better bond strength than OPC concrete. It was observed that the maximum bond strength of 12 mm ϕ bar of CFA20 is increased by18.56% and that of 16 mm ϕ is increased by 14.09%, CFA30 of 12 mm ϕ bar is increased by 50.34%

and that of 16 mm ϕ is increased by25.59% and CFA40of 12 mm ϕ bar is increased by 2.20% and that of 16 mm ϕ is increased by2.84% at full depth of specimen compared with OPC concrete.

Among all the FA mixes, mix containing 30% FA exhibited highest bond strength. The augmentation in the adhesive potency is attributed to the FA, which interacts with calcium hydroxide, a secondary product of cement hydration, to engender supplementary calcium silicate hydrate (C-S-H) gel. The application of this gel facilitates the filling of interstitial spaces between the cement paste and aggregate, thereby leading to an enhanced interfacial bond. The incorporation of mineral admixtures in conjunction with the highest possible cement content results in enhanced properties and densification of concrete. The study conducted laboratory experiments to collect concrete data, which was then subjected to mathematical analysis utilising statistical methods to predict the 28-day strength of concrete. The prediction models were based on the mix proportioning elements as the variables.

3.2 Silica Fume binary mix

Figure 3 show that the variations of maximum bond strength with different percentage replacement of cement by SF.It was observed that the maximum bond strength of 12 mm ϕ bar of CSF5 is increased by 57.22% and that of 16 mm ϕ is increased by 33.38%, CSF7.5of 12 mm ϕ bar is increased by 59.42% and that of 16 mm ϕ is increased by 47.15% and CSF10 of 12 mm ϕ bar is increased by 64.64% and that of 16 mm ϕ is increased by 63.77% at full depth of specimen compared with OPC concrete.Among all the SF mixes, mix containing 10% SF exhibited highest bond strength.

The augmentation in bond strength is attributed to the presence of SFs possessing a substantial surface area, thereby facilitating an increased surface area for the reaction with calcium hydroxide. This leads to a significant quantity of calcium-silicate-hydrate gel generation. The minute size of SF particles enables them to occupy the interstitial spaces between the comparatively larger aggregate particles, thereby leading to an enhancement in the packing density. Enhancement of the interfacial adhesion between the cement paste and aggregate leads to a consequent increase in the overall strength of the bond.

3.3 Ternary concrete mixes

Figure 4 show that the variation of maximum bond strength of ternary concrete mixes. It was observed that the maximum bond strength of 12 mm ϕ bar of CFA20SF5 is increased by 89.95% and that of 16 mm ϕ is increased by 46.76%, CFA30SF5of 12 mm ϕ bar is increased by 66.98% and that of 16 mm ϕ is increased by 37.01% and CFA40SF5of 12 mm ϕ bar is increased by 61.48% and that of 16 mm ϕ is increased by 21.73% at full depth of specimen compared with OPC concrete. The maximum bond strength of 12 mm ϕ bar of CFA20SF7.5 is increased by 119.66% and that of 16 mm ϕ is increased by 76.34%, CFA30SF7.5 of 12 mm ϕ bar is increased by 129.43% and that of 16 mm ϕ is increased by 80.46% and CFA40SF7.5 of 12 mm ϕ bar is increased by 88.85% and that of 16 mm ϕ is increased by 42.50% at full depth of specimen compared with OPC concrete.

The maximum bond strength of 12 mm ϕ bar of CFA20SF10 is increased by 103.30% and that of 16 mm ϕ is increased by 61.48%, CFA30SF10of 12 mm ϕ bar is increased by 68.50% and that of 16 mm ϕ is

increased by 50.48% and CFA40SF10 of 12 mm ϕ bar is increased by 74.55% and that of 16 mm ϕ is increased by 27.09% at full depth of specimen compared with OPC concrete. In all ternary concrete mixes, mix containing 30% FA and 7.5% SF exhibited highest bond strength. Novel concretes are produced through the partial or complete substitution of cement with SCMs, as well as the use of appropriate materials for sand and aggregates. Additionally, mineral or chemical admixtures are incorporated into the mixture..

3.4 Response surface method of bond strength

A statistical and mathematical technique known as response surface method is used to optimise and evolve issues when various influencing variables have an impact on the result variables. When a large number of factors strongly influence output parameters, the correlations between groups of independent variables can be easily found and effectively used. The independent variables were cement (X1), FA (X2), and SF (X3), and the bond strength response was calculated for bar diameter 12mm and 16mm i.e, f $bs_{12}$and f bs_{16}. The accuracy can be determined with the use of R^2. The relationship between progression variables and responses is investigated using a collection of statistical models and its evaluation procedure, known as analysis of variance. Table 2 shows that the model was very suitable because the P-value was less than 0.005.

Table 2
Analysis of Variance for f bs_{12} and f bs_{16}

Source	Bond strength(f bs_{12})			Bond strength(f bs_{16})		
	DF	F-Value	P-Value	DF	F-Value	P-Value
Model	5	10.77	0.001	5	12.74	≤ 0.001
Linear	2	14.77	0.001	2	19.92	≤ 0.001
X_1	1	28.88	≤ 0.001	1	39.76	≤ 0.001
X_2	1	25.13	0.001	1	38.27	≤ 0.001
Square	3	6.03	0.013	3	7.01	0.008
X_1*X_1	1	0.00	0.980	1	0.78	0.397
X_2*X_2	1	2.91	0.119	1	1.85	0.204
X_3*X_3	1	7.73	0.019	1	3.66	0.085

The model response is accurate, as the variation between the predicted R^2 and the adjustable R^2 of f bs_{12} and f bs_{16} was 13% and 17% which was less than 20%. Moreover, the R^2values of f bs12 and f bs16 were

84.34% and 86.43%, respectively. The correlation between predicted and experimental results is represented in Figs. 5 and 6.

The correctness of the model could be validated by means of F-value of the models, and its significant based on higher values of F. From Table 2, we can see the F values of 28.88 and 39.76, in the responses of fbs_{12} and fbs_{16}, respectively, indicating that the models are more considerable. Concrete is the most adaptable building material because it can be constructed to resist the toughest situations and take on the most inventive shapes. With the aid of innovative chemical admixtures and extra cementation materials, engineers are continuously pushing the boundaries to improve performance.

Concrete's splitting tensile strength is mostly influenced by the quality of its paste. Fine aggregate characteristics influence the quality of paste and the interfacial of transition zone. The growth of concrete's split tensile strength is comparable to its compressive strength. Different ages of curing in concrete have an effect on the paste's quality and its tensile strength. The increase in porosity and the distribution of pores are the primary causes of the reduced splitting tensile strength of concrete with different ageing. The conditions and kinds of cure highly affected the resistance to indirect tension. Moreover, the concrete's brittleness renders it extremely weak in stress [23–24].

4. Microscopic study of concrete paste

Using a Rigaku D/MAX-2400 diffractometer with Cu-K radiation emission at 40mA and 40kV, the X-ray diffraction (XRD) measurement of a building material was evaluated. Using the Scherrer Formula, the standard crystallite size (d) of the building materials was calculated from the line growth of high excessive reflection. On a Zeiss EVO 18 (SEM) instrument, the scanning electron microscopy (SEM) images of a building material were measured [25–26].

4.1 X-ray diffraction (XRD) study

The OPC mix diffractogram (Fig. 7) exhibits a considerable number of well-defined and distinct peaks of quartz, ettringite, CSH, and calcite. The existence of CSH and ettringite is indicative of their role in bolstering the concrete's strength. The identification of quartz and calcite peaks suggests the existence of crystalline silica and calcium carbonate, respectively, serving as inactive additives in the concrete. In addition to these minerals, the diffractogram of ordinary Portland cement (OPC) concrete also reveals the presence of peaks corresponding to portlandite. The identification of calcium hydroxide in OPC concrete is supported by the detection of the peaks of portlandite. Calcium hydroxide is generated through the process of cement hydration and exhibits solubility in water. The excessive production of calcium hydroxide has the potential to generate empty spaces within the concrete. It is a well-established fact that FA and SF contain a higher proportion of silica, resulting in an augmented quantity of crystalline silica (quartz), as depicted in Figs. 7 and 8. Additionally, the process of self-hydration in FA and SF results in the production of calcium carbonate, leading to an increase in the intensity of calcite as the amount of FA and SF increases [27–30].

In the XRD diffraction model of cement building materials, the crystalline portion of the material is represented by narrower peaks, while the amorphous portion of fibers is represented by larger peaks. It exhibits a broad peak at 2θ, where the values of 21.16 and 27.45 were associated by a Face-cantered cubic structure. OPC materials' crystallite size was 20.84 nm. Then, it is discovered that fibers diffraction patterns contain low crystalline content (amorphous). In the cement construction materials, alite, belite, and pentlandite were detected. The peak indicates that the presence of mixed $CaCO_3$, Al_2O_3, SiO and ZnO components. The surface of materials relates more to the accessibility of highly beneficial groups and bonds on the surfaces of construction materials [31–32].

4.2 Scanning electron microscopy (SEM) study

The purpose of obtaining SEM micrographs of concrete paste samples is to investigate the configuration of various hydration products, including CSH gel, ettringites, calcium hydroxide, and un-hydrated cement, FA, and SF particles within the concrete paste sample. The image of the OPC concrete mix (as shown in Fig. 9) reveals that the distribution of CSH formation is widespread. Moreover, the examination reveals the existence of calcium hydroxide crystals and the occurrence of pores and voids within the specimen [33–34]. The CFA30 mixture exhibits a reduction in CSH formation, which can be attributed to the slower hydration process of FA, as depicted in Fig. 10. The results obtained from the mixture of CSF10 and CFA30SF7.5 (Fig. 10) indicates that the concrete sample possesses a denser microstructure in comparison to that of CFA30. This can be attributed primarily to the filling of fine SF particles. As seen in the SEM micrograph, the particles of the building material were a combination of coarse, semi-coarse, and fine sizes, resulting from the use of (CFA10 mix and CFA30 mix), CFA30 mix and CFA30SF7.5 mix respectively [35–38].

The objective of capturing SEM micrographs of concrete paste samples is to analyse the organisation of various hydration products, including CSH gel, ettringites, calcium hydroxide, and un-hydrated cement, FA, and SF particles within the concrete paste sample. The concrete mix containing Ordinary Portland Cement (OPC) exhibits a dispersed distribution of Calcium Silicate Hydrate (CSH) throughout the visual representation depicted in Fig. 9. Furthermore, the examination of the sample reveals the existence of calcium hydroxide crystals, as well as the occurrence of pores and voids, as documented in references [33–34]. The CFA30 mixture exhibits a reduction in CSH formation, which can be attributed to the sluggish hydration of FA, as depicted in Fig. 10. The results depicted in Fig. 10 indicate that the compact microstructure of the concrete specimen is more pronounced in the CSF10 and CFA30SF7.5 blend, in contrast to the CFA30 mixture. This can be attributed to the effective filling of the fine SF particles. The building material particles, as evidenced by the SEM micrograph, exhibited a heterogeneous distribution of sizes, encompassing coarse, semi-coarse, and fine dimensions. This was attributed to the utilisation of CFA10 mix and CFA30 mix, CFA30 mix, and CFA30SF7.5 mix, as reported in references [35–38].

Changes in the composition and similarity of cement particles have also resulted from the presence of different combinations in the building materials. From SEM analysis, the similarity and shape of building material particles were discovered. The surface of the texture has fissures, as well as a heterogeneous

and mixed morphology with a strong porous configuration of varying sizes [39–40]. Concrete is an instantaneously hardening composite material made of fine and coarse particles linked together with liquid cement (cement paste). In the past, lime-based cement binders like lime putty were frequently employed, although rarely in conjunction with other hydraulic cements like Portland or calcium aluminates cement. Non-cementation forms of concrete exist with various techniques of particle binding, including asphalt concrete material with a bitumen binder, which is highly used for road surfaces, and polymer concretes with polymer binder [41–43].

5. Conclusion

The present study examines the bond performance of distorted steel bars that are embedded in binary and ternary concrete through experimental means. The principal findings of this investigation can be succinctly outlined as follows:

1. At the full depth of the embedment length, the interface between the steel and concrete exhibited adequate contact area, resulting in the failure of the specimen due to concrete splitting.
2. The binary and ternary concrete exhibited greater pull-out strength compared to OPC concrete for both bar diameters (ϕ = 12 and 16 mm).
3. The cohesive force of the binary concrete mixes containing FA exhibits a higher strength than that of the OPC concrete.
4. The highest bond strength was observed in binary concrete mixes containing 30% FA and 10% SF.
5. The ternary concrete mixture containing 30% FA and 7.5% SF demonstrated superior bond strength compared to both OPC and other blended concrete mixtures.

Declarations

Funding statement

This research received no specific grant from any funding agency in the public, commercial, or not-for-profit sectors.

Acknowledgements

The authors are thankful for the support from all the faculty members and lab in charges of Civil Engineering Department, Gudlavalleru Engineering College.

Declaration of Competing Interest

The authors declare no conflict of interest.

Data Availability Statement

The statements in the paper are properly cited in the manuscript and no additional data is available.

References

1. ACI Committee 232. Use of fly ash in concrete (ACI 232.2R-03). Farmington Hills, MI: American Concrete Institute; 2003.
2. ACI Committee. 2003. Bond and development of straight reinforcing bars in tension. ACI 408R-03),American Concrete Institute, Farmington Hills, Mich 48.
3. Ahmed, S., Alsayed, S.H., Al-Kattan, M.and Abdel-Mohti, A. 2018. Effect of fly ash and silica fume on the bond strength between concrete and steel reinforcement bars. Construction and Building Materials 188, 216-224. doi: 10.1016/j.conbuildmat.2018.07.138
4. Alonzo, O., Barringer, W.L., Barton, S.G., Bell, L.W., Bennett, J.E., Boyle, M. and Dixon, D.E. 1993. Guide for selecting proportions for high-strength concrete with portland cement and fly ash. ACI Mater J. 90(3), 272-283.
5. de Almeida Filho, F.M., Debs, M.K. and Debs, A.L.H. 2008. Bond-slip behaviour of self-compacting concrete and vibrated concrete using pull-out and beam tests. Materials and Structures 41(6), 1073-1089.
6. Al-Swaidani, A.M., Almusallam, T H. and Tagnit-Hamou, A. 2015. Bond strength of reinforcing steel bars to concrete with silica fume. International Journal of Concrete Structures and Materials, 9(3), 319-329.
7. Al-Swaidani, A.M., Almusallam, T.H. and Taha, R. 2013. Bond strength of steel fibre-reinforced concrete with silica fume. ACI Materials Journal 110(3), 295-304. doi: 10.14359/51684608
8. Argiz, C., Moragues, A. and Menéndez, E. 2018. Use of ground coal bottom ash as cement constituent in concretes exposed to chloride environments. Journal of Cleaner Production 170, 25-33.
9. ASTM 618-94a. 1995. Standard specification for coal fly ash and raw or calcined natural pozzolan for use as a mineral admixture in portland cement concrete. In: Annual book of ASTM standards, American Society for Testing and Materials 4(12), 304–306.
10. Barluenga, G., Oller, E., Etxeberria, M. and Barragan, B. 2012. The influence of fly ash and silica fume on the bond strength of steel fiber reinforced concrete. Construction and Building Materials, 35, 236-244.
11. Azimi, M., Pourkhorshidi, A.R. and Jahangiri, M. 2018. The effect of fly ash and silica fume on the bond strength between steel bars and concrete. Journal of Civil Engineering and Management, 24(6), 465-474.
12. Cross, D., Stephens, J. and Vollmer, J. 2005. Structural applications of 100 percent fly ash concrete. Montana State University, Bozeman, *MT*.
13. Berry, E.E., Hemmings, R.T., Zhang, M.H., Cornelius, B.J. and Golden, D.M. 1994. Hydration in high-volume fly ash concrete binders. Materials Journal, 91(4), 382-389.
14. De Brito, J. and Saikia, N. (2012). Recycled aggregate in concrete: use of industrial, construction and demolition waste. Springer Science & Business Media.

15. Bilodeau, A. and Malhotra, V.M. 2000. High-volume fly ash system: concrete solution for sustainable development. Materials Journal 97(1), 41-48.
16. Foroughi, A.A., Dilmaghani, S. and Famili, H. 2008. Bond strength of reinforcement steel in self-compacting concrete.Advances in Structural Engineering 15(12), 1369-1380.
17. Elchalakani, M., Heidarpour, A. and Zhao, X. (2018). Bond strength between high-strength steel bars and concrete containing silica fume. Magazine of Concrete Research, 70(6), 309-320. doi: 10.1680/jmacr.16.00666
18. Kim, J.K., Lee, H.K., and Oh, B.H. 2015. Effect of fly ash and silica fume on interfacial bond strength of concrete with different aggregates. Construction and Building Materials 92, 144-152. doi: 10.1016/j.conbuildmat.2015.05.007
19. Lee, H.K., Kim, J.K. andOh, B.H. 2018. Bond strength of fibre-reinforced concrete with fly ash and silica fume. Construction and Building Materials, 188, 346-355. doi:10.1016/j.conbuildmat.2018.07.231
20. Lee, H.K., Kim, J.K., Park, M.H. and Oh, B.H. 2015. Bond strength of high-performance concrete with silica fume and high-range water-reducing admixture. Construction and Building Materials, 90, 132-140. doi: 10.1016/j.conbuildmat.2015.05.033
21. Gopalakrishnan, S., Lakshmanan, N., Rajamane, N., Krishnamoorthy, T., Neelamegam, M., Chellappan, A. and Sabitha, D. 2005. Demonstration of utilising high volume fly ash based concrete for structural applications. A report prepared for confederation of Indian industry *(CII),* India.
22. Han, D., Kim, D., Park, C. and Choi, W. 2019. Bond strength of fiber-reinforced concrete containing fly ash and silica fume. Sustainability, 11(8), 2352. doi: 10.3390/su11082352
23. Hosseini, S.J.A., Koushfar, K., Baharuddin, A., Rahman, A. and Razavii, M. 2014. Harmony of bond behaviour in reinforced concrete, part two. Cement WapnoBeton, 11(6), 384-395.
24. Hosseini, S.J., Koushfar, K., Rahman, A.B.A. and andRazavi, M. 2014. The bond behaviour in reinforced concrete, state of the art. Cement WapnoBeton, 11(2), 93-105.
25. Lu, X., Jiang, Y., Sun, Y. and Wang, D. 2017. Influence of super plasticizers on bond strength between fiber-reinforced concrete and steel bar. Journal of Materials in Civil Engineering, 29(8), 04017063. doi: 10.1061/(ASCE)MT.1943-5533.0001911
26. Marinković, S., Dragaš, J., Ignjatović, I. and Tošić, N. 2017. Environmental assessment of green concretes for structural use. Journal of Cleaner Production 154, 633-649.
27. Naik, T.R., Singh, S.S., Sivasundaram, V. and Energy, M. 1989. Concrete compressive strength, shrinkage and bond strength as affected by addition of fly ash and temperature. The University of Wisconsin–Milwaukee, Milwaukee, WI.
28. Prasad, M.L.V., Loksesh, G., Ramanjaneyulu, B., Venkatesh, S. and Mousumi, K. 2017. Glass fiber effect on mechanical properties of Eco-SCC AIP Conference Proceedings 1859, 020012.
29. Jadham, R., Bharadwaj, A. and Pastariya, S. 2020. Experimental investigation on quarry dust as a partial replacement of sand for M-40 grade concrete. International Research Journal of Engineering and Technology 7(11), 978-981.

30. Hanifı, B., Hasan K. and Salih, Y. 2007. Influence of marble and limestone dusts as additives on some mechanical properties of concrete. Academic Journals 2(9), 372-379.
31. Oyekan G.L. and Kamiyo O.M. 2008. Effects of granite fines on the structural and hygro-thermal properties of sand Crete blocks. Nigeria journal of Engineering and Applied sciences 3(3), 735-741.
32. Kunther, W., Lothenbach, B. and Skibsted, J. 2015. Influence of the Ca/Si Ratio of the C-S-H Phase on the Interaction with Sulfate Ions and Its Impact on the Ettringite Crystallization Pressure. Cement and Concrete Research 69, 37-49.
33. Danso, H. 2020. Influence of Plantain Pseudostem Fibres and Lime on the Properties of Cement Mortar. Advances in Materials Science and Engineering Article ID: 4698603.
34. Dhir, R.K., Hewlett, P.C. and Dyer, T.D. 1995. Durability of 'self-cure' concrete. Cement and Concrete Research 25(6), 1153-1158.
35. Botero, C.A., Jimenez-Piqué, E., Martín, R., Kulkarni, T., Sarin, V.K. and Llanes, L. 2014. Nano indentation and Nanoscratch properties of mullite-based environmental barrier coatings: Influence of chemical composition-Al/Si ratio. Surface and Coatings Technology 239, 49-57.
36. Bentz, D.P. and Jensen, O.M., 2004. Mitigation strategies for autogenous shrinkage cracking. Cement and Concrete Composites 26(6), 677-685.
37. Kumar, R. and Bhattacharjee, B. 2003. Porosity, pore size distribution and in situ strength of concrete. Cement and concrete research 33(1), 155-164.
38. Mehta, P.K. and Monteiro, P.J.M. 2014. Concrete: microstructure, properties and materials. McGraw-Hill Education.
39. Akcay, B. and Tasdemir, M.A. 2012. Mechanical behaviour and fibre dispersion of hybrid steel fiber reinforced self-compacting concrete. Construction and Building Materials 28(1), 287-293.
40. Long, G., Gao, Y. and Xie, Y. 2015. Designing more sustainable and greener self-compacting concrete [R]. Construction and Building Materials 84, 301-316.
41. Provis, J.L., Palomo, A. and Shi, C. 2015. Advances in understanding alkali-activated materials. Cement and Concrete Research, *78*, 110-125.
42. Sarika, P.R., Mini, K.M., Nair, S. and Mathew, M.K. 2016. Interfacial bond strength of concrete with fly ash and silica fume. Construction and Building Materials 127, 105-111. doi: 10.1016/j.conbuildmat.2016. 10.031
43. Wang, W., Li, W., Li, Y., Li, Y. and Liu, S. 2018. Effect of fly ash and silica fume on interfacial bond strength and microstructure of concrete with different curing methods. Construction and Building Materials 161, 188-199. doi: 10.1016/j.conbuildmat.2017.11.063.

Figures

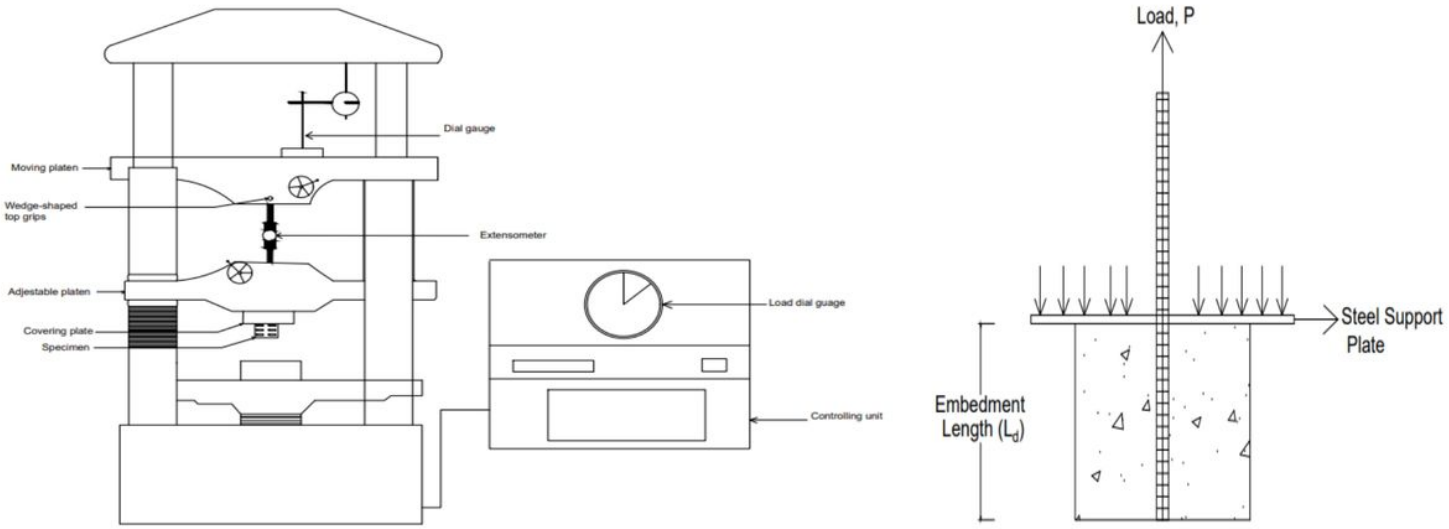

Figure 1

Sectional view of UTM and Pull-out Specimen

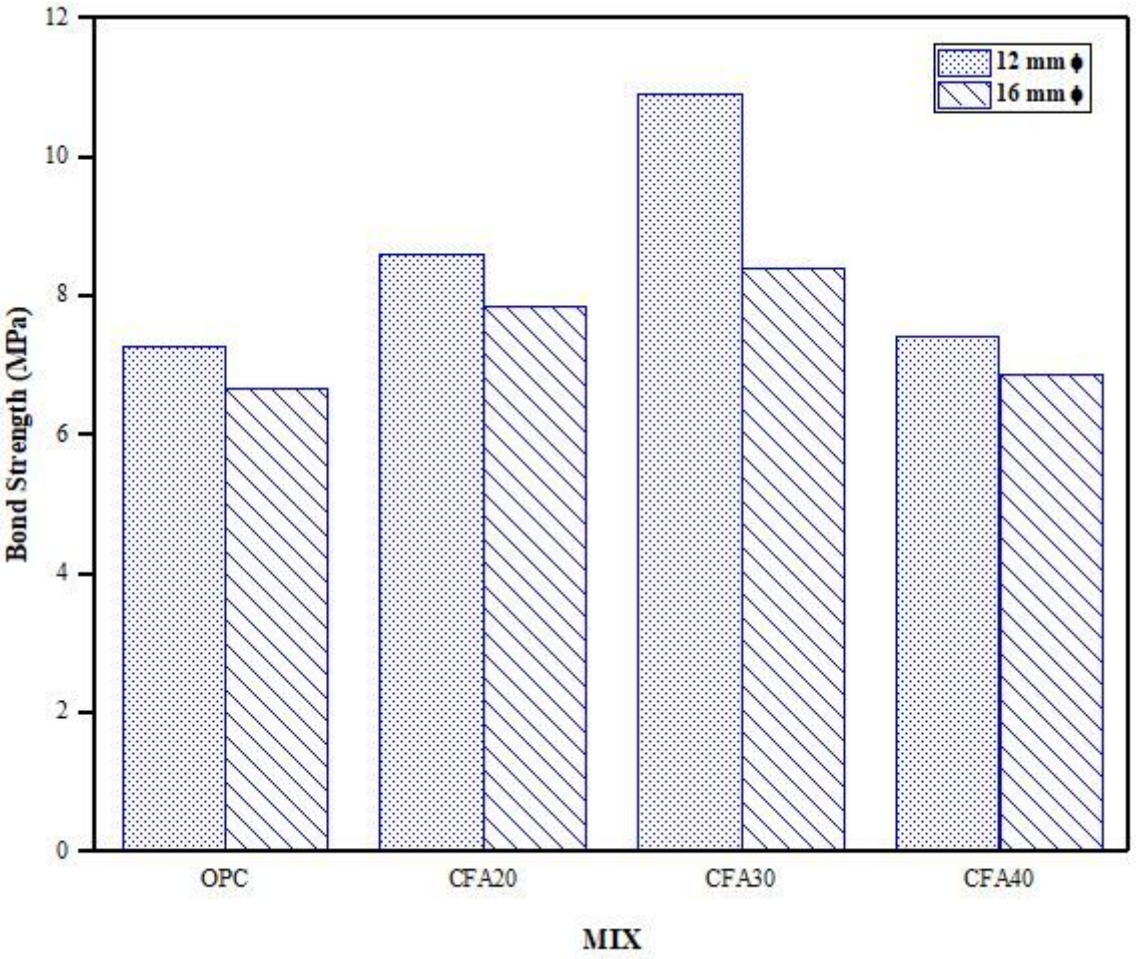

Figure 2

Bond Strength of CFA mixes at various bar diameters

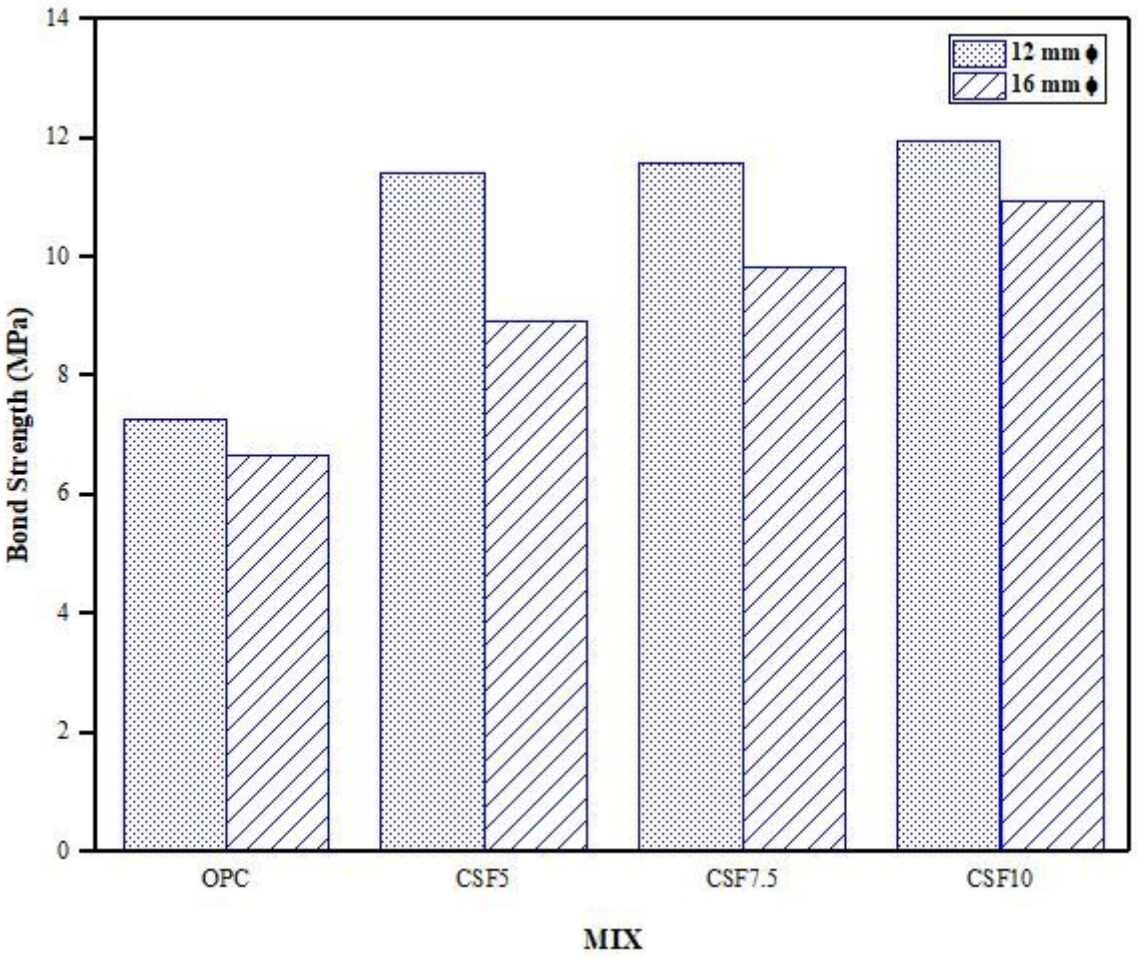

Figure 3

Bond Strength of CSF mixes at various bar diameters

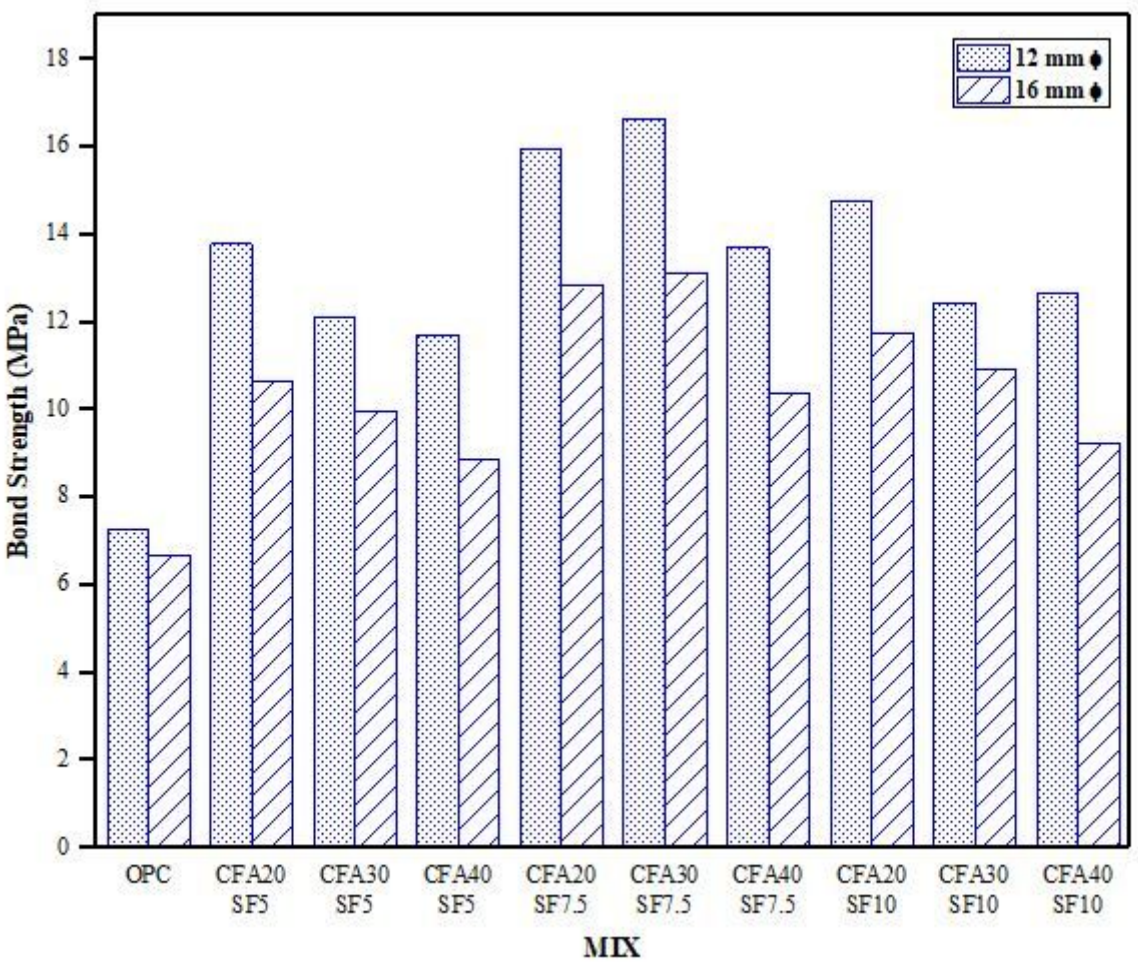

Figure 4

Bond Strength of CFASF mixes at various bar diameters

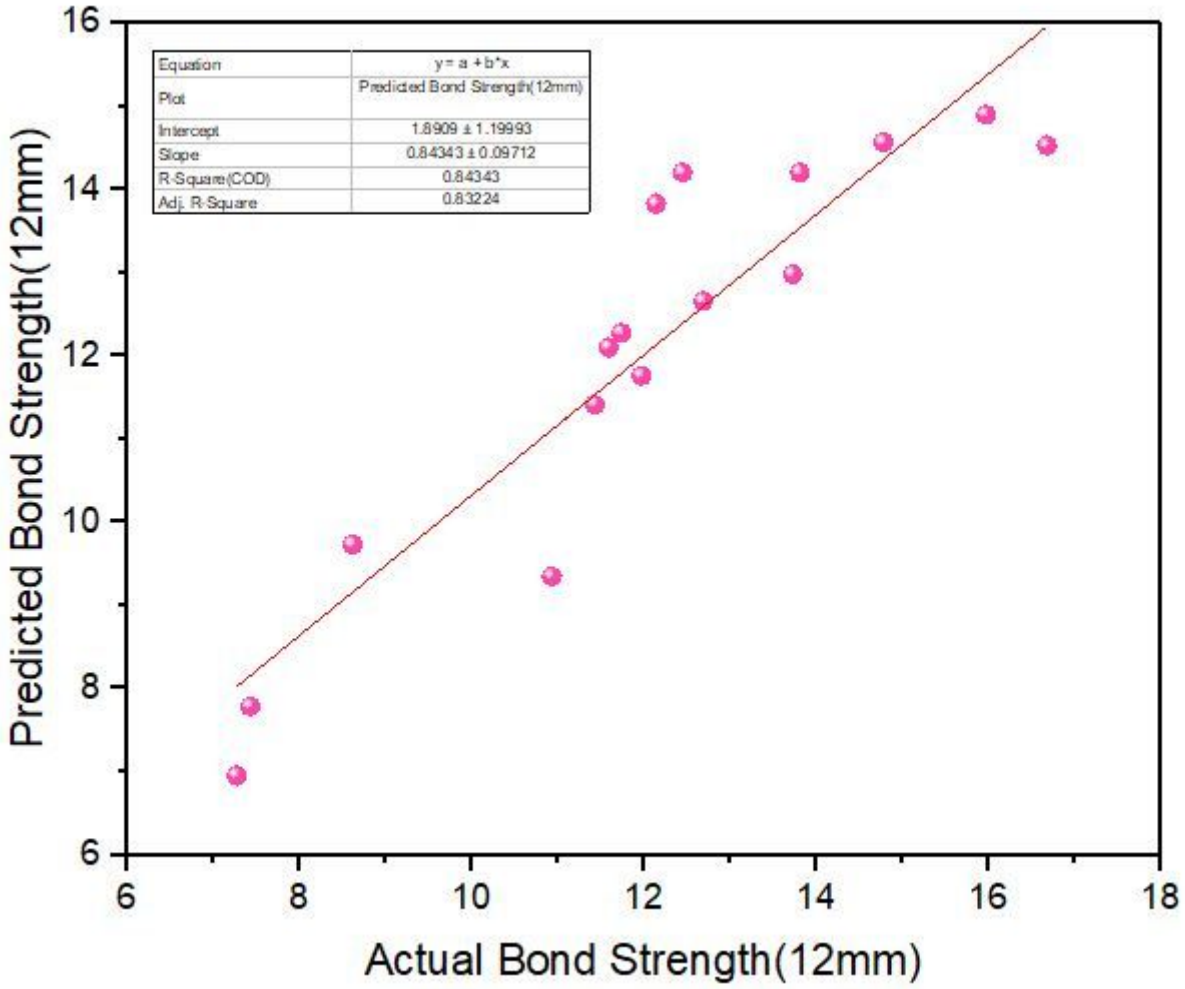

Figure 5

Predicted and actual values of bond strength (12mm φ)

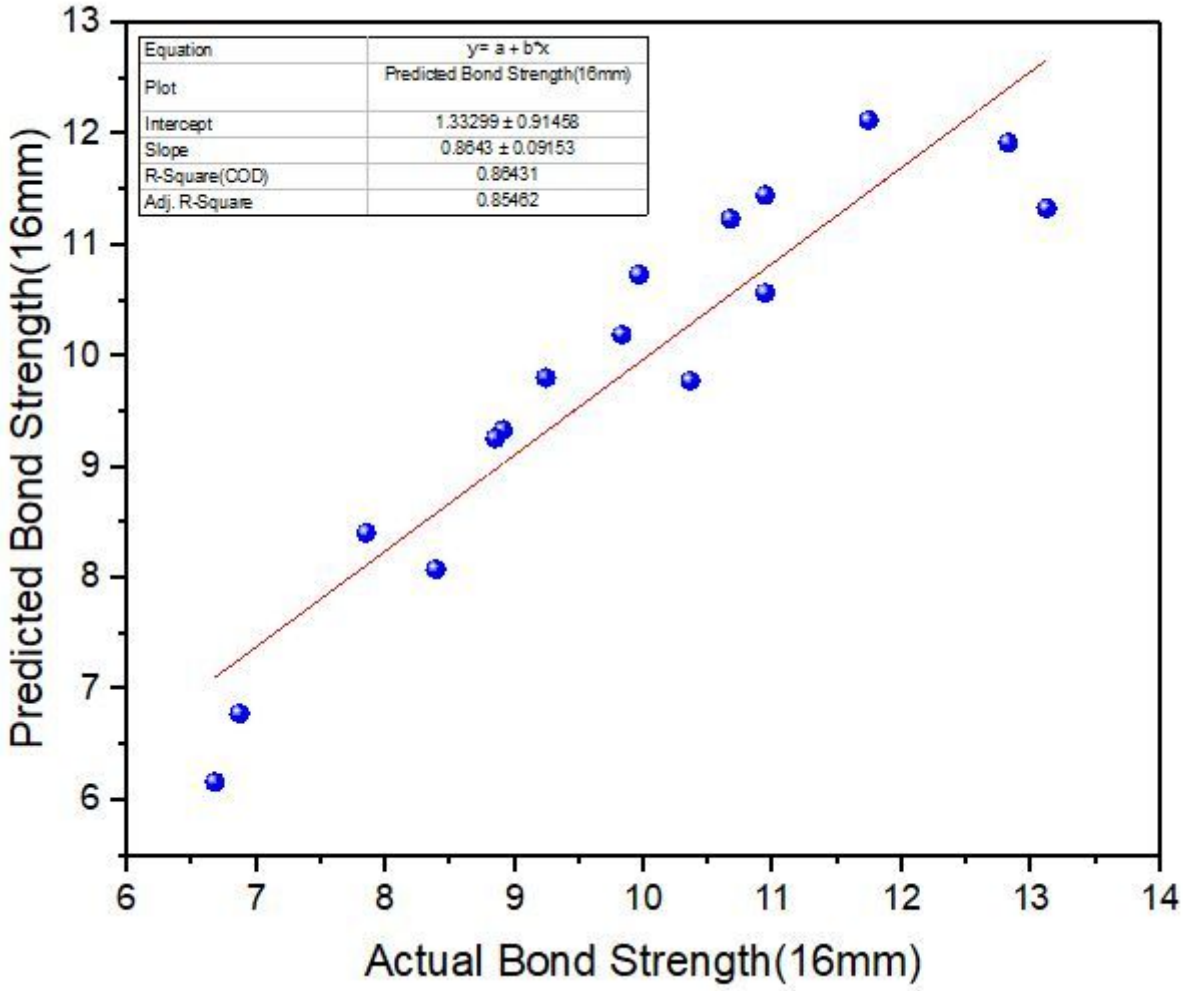

Figure 6

Predicted and actual values of bond strength (16mm φ)

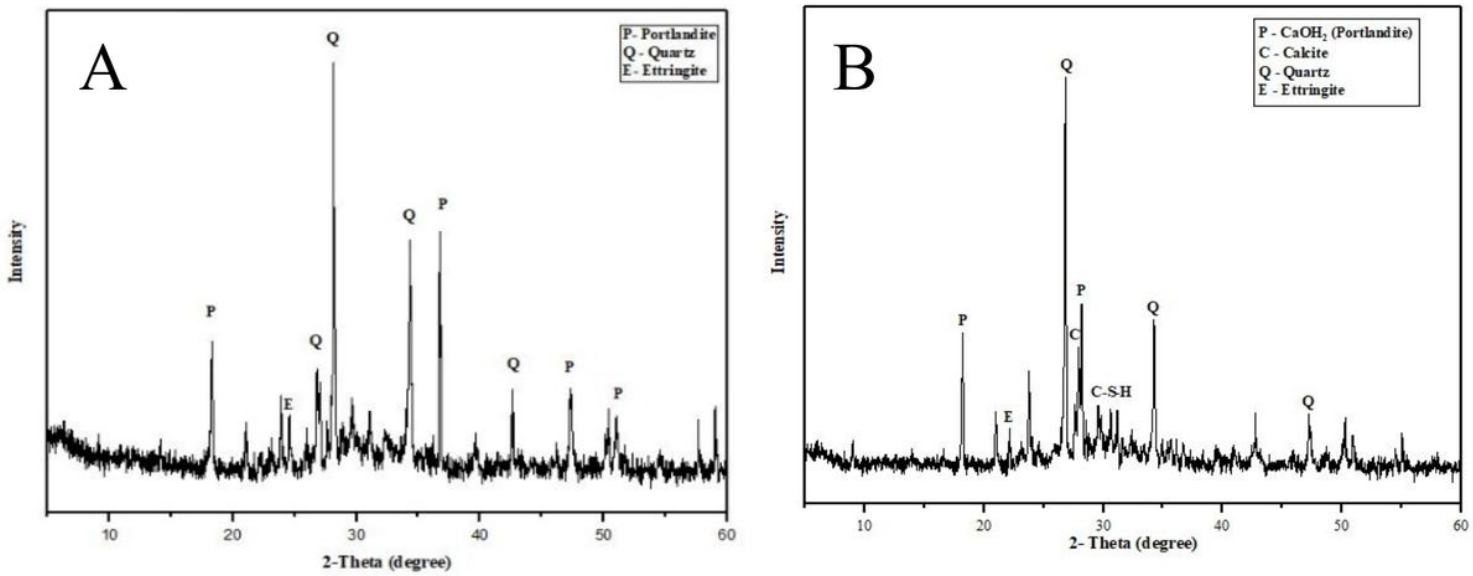

Figure 7

(A) XRD of OPC mix and (B) XRD of CFA30 mix

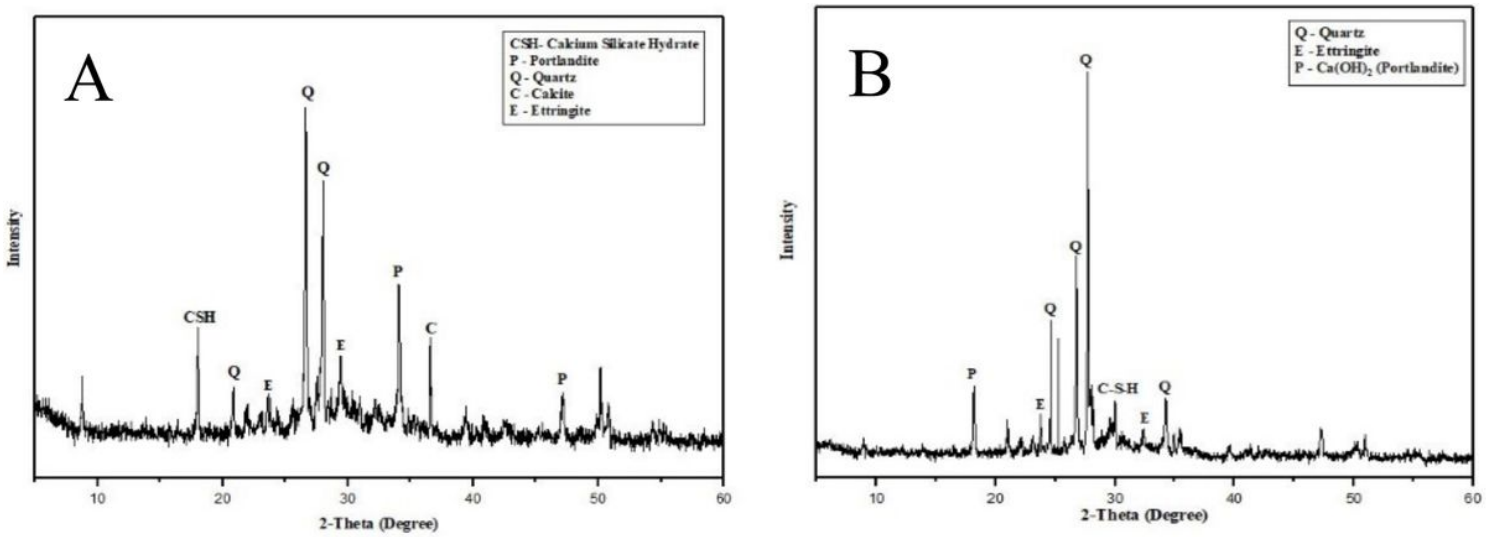

Figure 8

(A) XRD of CSF10 mix **and (B)** XRD of CFA30SF7.5 mix

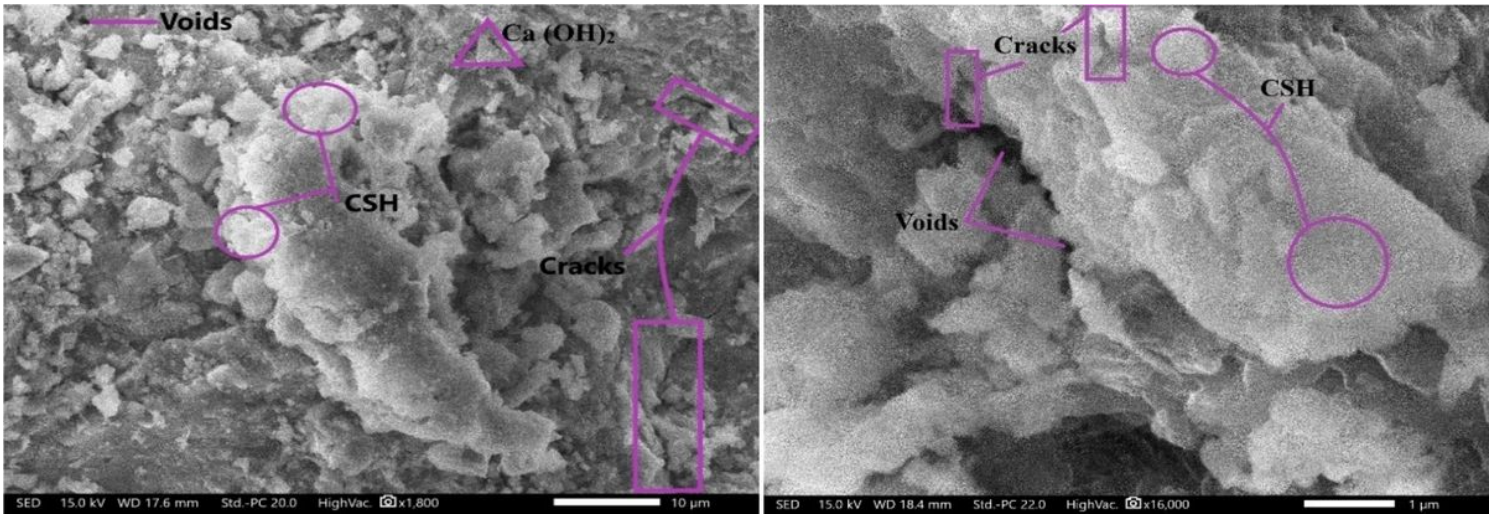

Figure 9

(A) SEM of OPC mix **and (B)** SEM of CFA30 mix

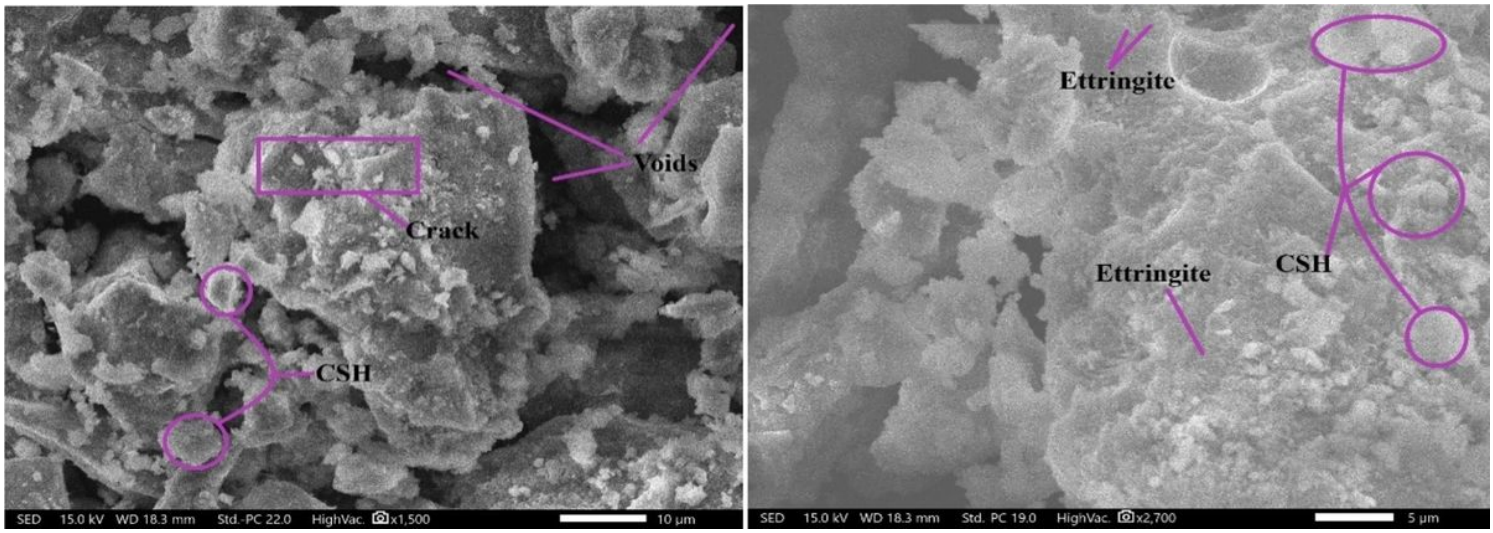

Figure 10

(A) SEM of CSF10 mix and (B) SEM of CFA30SF7.5 mix